

# Effect of thermal annealing on crystallinity and mechanical strength of textile glass and carbon fiber reinforced in situ polymerized $\epsilon$ -caprolactam parts

Kentaro Taki<sup>1</sup>  · Hiroto Suenaga<sup>2</sup> · Hiroshi Ito<sup>2,3</sup>

Received: 26 January 2017 / Accepted: 3 February 2017 / Published online: 10 February 2017  
© Springer-Verlag Berlin Heidelberg 2017

**Abstract** Fiber reinforced thermoplastic (FRTP) is a promising material for automobiles, airplanes, construction, home appliances and so on. In situ polymerized polyamide (PA6) is a representative polymer material for FRTP. When  $\epsilon$ -caprolactam ( $\epsilon$ -CL) is polymerized in situ, the polymerization of  $\epsilon$ -CL and crystallization of PA6 occur simultaneously. The polymerization temperature is far below the melting temperature of PA6, and the obtained crystallinity and mechanical strength are far below those of a part prepared by injection molding. Thermal annealing is a practical approach to improve the crystallinity and mechanical properties. However, the effect of thermal annealing on the crystallinity and mechanical properties of FRTPs is still unclear. This study investigated the effect of thermal annealing on the crystallinity and mechanical properties of PA6, textile glass fiber reinforced PA6 (GF-PA6), and carbon fiber reinforced PA6 (CF-PA6) (40 vol%). The specimens were prepared by resin transfer molding with in situ polymerization of  $\epsilon$ -CL. PA6 was polymerized

in situ in a mold with and without fibers. The results indicated that the crystallinity, tensile modulus, and strength of PA6 were improved by thermal annealing. The crystallinity of GF-PA6 was not improved, but the tensile modulus and strength were slightly improved. The crystallinity of CF-PA6 decreased, but the tensile modulus and strength improved. The crystallinity showed a negative correlation to the tensile modulus and strength. Because the tensile modulus and strength of glass and carbon fibers are much higher than those of the crystalline phase of PA6, increasing the crystallinity had a limited effect.

## 1 Introduction

Carbon fiber reinforced thermoplastic (CFRTP) is a promising material for automobiles, airplanes, construction, home appliances and any parts that require high strength with low weight. In situ polymerized polyamide (PA6) is a representative polymer material for CFRTP that has low viscosity, a rapid polymerization time, and no byproducts. Resin transfer molding (RTM) is a practical process for realizing *in situ* polymerization of  $\epsilon$ -caprolactam ( $\epsilon$ -CL) and crystallization of PA6 to produce composites with glass fiber and carbon fiber fabrics in a mold (Zheng et al. 2002; Shojaei et al. 2003; van Rijswijk and Bersee 2007; Pillay et al. 2005; Ben et al. 2015).

Because PA6 is a semi-crystalline polymer, its crystallization is important for not only the RTM process but also its mechanical properties. However, there has been little discussion on its crystallization and mechanical properties.

In our previous study, when  $\epsilon$ -CL was polymerized in situ, the polymerization and crystallization occurred simultaneously, and a subsequent rise in viscosity was observed (Taki et al. 2016). Differential scanning

✉ Kentaro Taki  
taki@se.kanazawa-u.ac.jp

✉ Hiroshi Ito  
ihiroshi@yz.yamagata-u.ac.jp

Hiroto Suenaga  
tna77760@st.yamagata-u.ac.jp

<sup>1</sup> School of Natural System, Kanazawa University,  
Kanazawa 920-1192, Japan

<sup>2</sup> Department of Polymer Science and Engineering, Graduate  
School of Science and Engineering, Yamagata University,  
4-3-16, Jonan, Yonezawa, Yamagata 992-8510, Japan

<sup>3</sup> Department of Organic Materials Science, Graduate School  
of Organic Materials Science, Yamagata University, 4-3-16,  
Jonan, Yonezawa, Yamagata 992-8510, Japan

calorimetry during  $\epsilon$ -CL polymerization revealed superimposed peaks of crystallization and polymerization. The peaks were separated mathematically and examined to determine the rate parameters of polymerization and crystallization. The polymerization and crystallization rates were modeled with the Kamal model (Kamal and Ryan 1980) and generalized Avrami model (Ito et al. 1995), respectively. Increasing both the polymerization and crystallization increased the viscosity as well. The increase in viscosity was modeled with the modified Castro–Macosko model (Castro and Macosko 1980). This study revealed that the crystallization occurred during polymerization and that the crystallinity was limited by the degree of polymerization. To improve the crystallinity, the polymerization temperature needs to be increased. However, increasing the temperature causes  $\epsilon$ -CL to vaporize. Thus, the temperature must be far below the melting temperature. Then, the crystallinity becomes lower than the melt crystallization.

Haspel et al. reported a significantly lower interfacial shear strength with significantly lower formation of crystalline spherulites at the interfacial layer for GF-PA6 (Haspel et al. 2015). Durin et al. proposed a detailed model of crystallization in long-fiber PA6 composites (Durin et al. 2017). They incorporated a model for transcrystallinity on fiber surfaces. Yan et al. investigated the effect of thermal annealing on the mechanical properties of CF-PA6 at the macroscale and local scale (Yan et al. 2014). They prepared CF-PA6 by hand-press injection molding. The crystallinity, flexural modulus, and strength were improved when the annealing temperature was increased. However, their CF-PA6 became brittle as the  $\gamma$  phase crystallinity increased. Li et al. investigated the interfacial thickness, modulus, adhesion, and shear strength of CF-PA6 prepared from molten PA6 and carbon fibers (Li et al. 2016). When the annealing temperature was increased, the crystallinity and interface modulus were increased. Their study indicated that the thermal annealing was a promising approach for improving the mechanical properties of PA6, GF-PA6, and CF-PA6 prepared by RTM with in situ polymerization of  $\epsilon$ -CL. These previous studies focused on the

crystallization of PA6 that had not been prepared by in situ polymerization of  $\epsilon$ -CL.

In this study, the effect of thermal annealing on the crystallinity and mechanical properties of PA6, glass fiber reinforced PA6 (GF-PA6), and carbon fiber reinforced PA6 (CF-PA6) was investigated. PA6 was polymerized in situ in a mold with and without fibers. The tensile modulus, strength, and degree of crystallinity were measured, and their relationships were examined.

## 2 Materials and methods

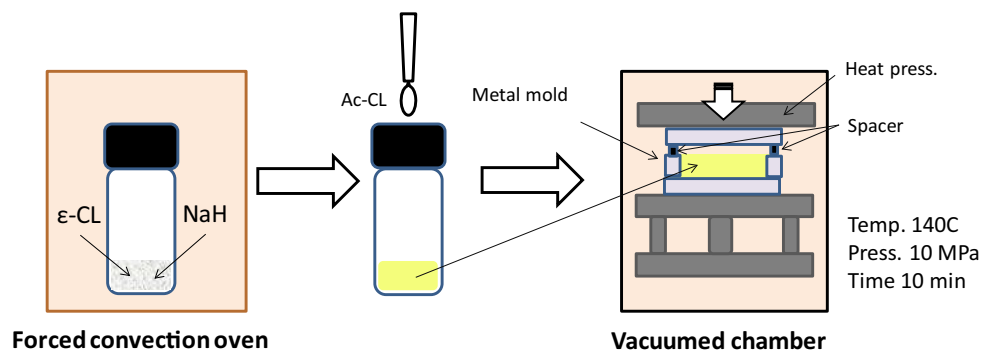
### 2.1 Materials

$\epsilon$ -CL (cat. 030-01125,  $T_m = 68$  °C, Wako Pure Chemical, Japan) was used as the monomer of PA6. Sodium hydride (NaH, cat. 452912, 60% dispersion in mineral oil, Sigma-Aldrich, USA) was used as the catalyst for polymerization. *N*-acetyl- $\epsilon$ -caprolactam (Ac-CL, cat. A0081, Tokyo Chemical Industry, Japan) was used as the activator for polymerization. The reagents were used without further purification. Sodium hydrate was used after the mineral oil was vaporized at room temperature. The reinforcing materials were a plain weaved glass fiber (GF) mat ( $54 \times 45$  mm<sup>2</sup>) and non-woven carbon fiber (CF) mat ( $50 \times 45$  mm<sup>2</sup>, TORAY). The volume percentages of the GF and CF were each 40%. Hereafter, the sample without a mat is designated as PA6, the sample with GF is designated as GF-PA6, and the sample with CF is designated as CF-PA6.

### 2.2 In situ polymerization

In situ polymerization was performed according to the sequence shown in Fig. 1. First, 0.089 g of NaH was obtained by drying the dispersed solution of NaH and placed into a glass vial. Then, 14 g of  $\epsilon$ -CL was added to the vial, and the vial was sealed. Each vial was heated in a forced convection oven for 30–35 min at 90 °C or for 20–25 min at 100 or 110 °C.  $\epsilon$ -CL and NaH were melted at these temperatures and mixed together. Ac-CL was then

**Fig. 1** In situ polymerization of  $\epsilon$ -CL



added to the vial immediately. In this study, the effect of the melt temperature on the crystallinity and mechanical properties was investigated by varying the temperature to 90, 100, and 110 °C.

The solution was poured in a round-shaped metal mold placed in a vacuumed heat press (IMC-11 FA, Imoto Machinery, Japan). The mold was pressed by the heat press at 10 MPa for 10 min. The polymerization of  $\epsilon$ -CL proceeded in the mold. The mold was preheated at 140 °C. The diameter and height of the space where the polymerization proceeded in the metal mold were 70 and 3 mm, respectively. When  $\epsilon$ -CL was polymerized with the reinforcing materials (i.e., GF and CF), the materials were preheated in the mold at 140 °C.

### 2.3 Thermal annealing

The in situ polymerization reached limited crystallinity because the polymerization had to proceed far below the melting temperature of PA6 to avoid the vaporization of  $\epsilon$ -CL. Thermal annealing is a practical way to increase the crystallinity. Two different types of thermal annealing were attempted.

First, thermal annealing was performed with a differential scanning calorimeter (DSC, DSC 8500, Perkin-Elmer, USA). A few milligrams of each polymerized sample was heated from 20 to 200 °C at 10 °C min<sup>-1</sup>. The temperature was kept for 1 h at 200 °C. To analyze the crystallinity, the temperature was decreased from 200 to 20 °C at 10 °C min<sup>-1</sup> and heated up to 270 °C at the same heating rate. This thermal annealing in the DSC was performed under a nitrogen flow of 20 mL min<sup>-1</sup>.

The second type of thermal annealing was performed on a mechanical testing specimen in a forced convection oven. A 7 × 45 × 3 mm<sup>3</sup> specimen was cut out from a molded circular disk. The specimen was heated at 200 °C for 1 h in a nitrogen flow.

### 2.4 Characterization

#### 2.4.1 Conversion and molecular weight

The polymerized samples were ground and dispersed in water to dissolve the residual  $\epsilon$ -CL for 48 h. The granules were collected with a filter and dried at 80 °C for 8 h. The weight loss was calculated by comparing each sample before and after being soaked in the water. The conversion was calculated as follows:

$$\text{Conversion (\%)} = W_a/W_b \times 100 \quad (1)$$

where  $W_a$  and  $W_b$  are the weights before and after the sample was soaked in water, respectively.

The number average and weight average molecular weights were measured by using gel permeation chromatography. The elution solvent was hexafluoroisopropanol (HFIP). The polystyrene standard was used.

#### 2.4.2 Thermal analysis

Thermal analysis was performed with the DSC. The heating rate was 10 °C min<sup>-1</sup>. The temperature range was 20–270 °C. The DSC was calibrated with indium. The crystallinity was calculated from the enthalpy of fusion of crystalline phase per gram with the reference value  $\Delta H_f = 230$  (J/g) (Blaine 2002). The peak of the fusion curve was measured for the fusion (melting) temperature.

#### 2.4.3 Mechanical testing

A flexural test was performed with a universal testing machine (Strograph VGS1-E, TOYOSEIKI, Japan). A three-point testing fixture with a supporting span of 40 mm was used. The crosshead speed was 2 mm min<sup>-1</sup>. The test was performed at room temperature. The typical specimen size was 7 × 45 × 3 mm<sup>3</sup>. Each specimen was dried at 80 °C in a vacuum chamber for at least 1 day before testing. At least three specimen were examined and obtained average and standard deviation for the error bar.

## 3 Results

### 3.1 Conversion and molecular weight

Table 1 presents the effect of the melt temperature on the conversion and molecular weight. Increasing the melt temperature or decreasing  $\Delta T$  (=polymerization temperature – melt temperature) increased the conversion, number-average-molecular weight, and weight-average-molecular weight. A small  $\Delta T$  reduced the time for the polymerization temperature (140 °C) to be reached. A small  $\Delta T$  meant that polymerization occurred at a higher temperature for a long time, which increased the conversion and molecular weights.

**Table 1** Effect of the melt temperature on the conversion and molecular weight

Melt temperature (°C)	$\Delta T$ (°C)	Conversion (%)	$\bar{M}_n$	$\bar{M}_w$
90	50	86	26,000	57,000
100	40	90	27,000	59,000
110	30	93	34,000	72,000

### 3.2 Crystallinity, flexural modulus, and strength

Table 2 summarizes the effect of thermal annealing on the fusion (melting) temperature, crystallinity, flexural modulus, and strength.

#### 3.2.1 PA6

Table 2 presents the effect of thermal annealing at 200 °C on the fusion temperature and crystallinity. The thermal annealing increased the fusion temperature by about 10 °C and the crystallinity by about 20%. The fusion temperature reached or was close to the value in the literature for PA6 (i.e., 220 °C) (Brandrup et al. 2003). The melt temperature showed no distinct trend in its effect on the fusion temperature and crystallinity. Because the crystallinity was increased by thermal annealing, the specimen for mechanical testing was thermally annealed at the same temperature.

Figure 2 shows the effect of thermal annealing on the flexural modulus and strength. Thermal annealing improved the flexural modulus and strength. The impact was more pronounced on the flexural modulus than on the strength. As the crystallinity increased by thermal annealing, the

crystallinity was found to affect the modulus rather than the strength.

#### 3.2.2 GF-PA6

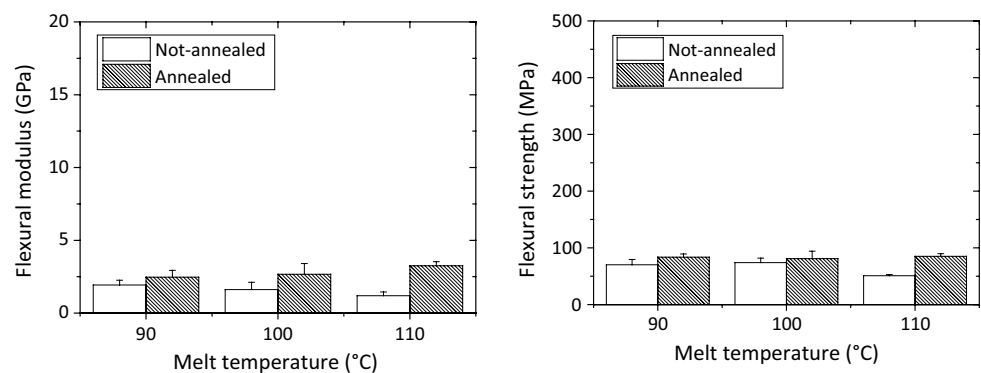
Table 2 presents the effect of thermal annealing on the fusion temperature and crystallinity of GF-PA6. In contrast to the results for PA6, thermal annealing was less effective at improving the fusion temperature and crystallinity. The fusion temperature increased by 3 °C at most. The crystallinity decreased or was equal to the non-annealed samples.

Figure 3 shows the effect of thermal annealing on the flexural modulus and strength. The sample with a melt temperature of 90 °C showed a similar flexural modulus. Both samples with melt temperatures of 100 and 110 °C showed an improvement in the modulus with thermal annealing. The strengths of both the 90 and 100 °C samples decreased, and that of the 110 °C sample increased. Again, thermal annealing had less effect on these mechanical properties. It was interesting to observe that thermal annealing is not a straightforward method for improving both the crystallinity and mechanical properties.

**Table 2** Effect of thermal annealing on the fusion temperature, crystallinity, flexural modulus, and strength

Sample	Melt temperature (°C)	Fusion temperature, $T_f$ (°C)		Crystallinity, $\chi$ (%)		Flexural modulus (GPa)		Flexural strength (MPa)	
		Not annealed	Annealed	Not annealed	Annealed	Not annealed	Annealed	Not annealed	Annealed
PA6	90	210	219	11	39	1.93 ± 0.33	2.47 ± 0.47	70.2 ± 9.4	83.7 ± 5.5
PA6	100	213	220	22	41	1.62 ± 0.50	2.67 ± 0.74	73.9 ± 7.9	81.0 ± 13.2
PA6	110	211	219	24	38	1.19 ± 0.26	3.25 ± 0.28	50.9 ± 2.1	85.1 ± 4.6
GF-PA6	90	213	214	32	30	5.48 ± 0.81	5.45 ± 0.86	120.6 ± 20.3	111.6 ± 8.7
GF-PA6	100	213	216	39	33	7.27 ± 0.65	8.26 ± 2.28	116.8 ± 7.7	111.2 ± 23.8
GF-PA6	110	214	216	34	34	4.09 ± 0.59	5.58 ± 0.21	112.8 ± 10.8	134.0 ± 11.0
CF-PA6	90	212	215	39	39	10.58 ± 1.94	12.5 ± 1.38	225.1 ± 31.9	243.4 ± 51.1
CF-PA6	100	212	215	42	37	12.31 ± 0.77	13.9 ± 4.15	216.5 ± 26.8	245.5 ± 70.4
CF-PA6	110	211	216	44	43	8.34 ± 4.07	8.93 ± 2.34	127.4 ± 13.5	139.1 ± 116.8

**Fig. 2** Effect of thermal annealing on the flexural modulus (left) and strength (right) of PA6



**Fig. 3** Effect of thermal annealing on the flexural modulus (left) and strength (right) of GF-PA6

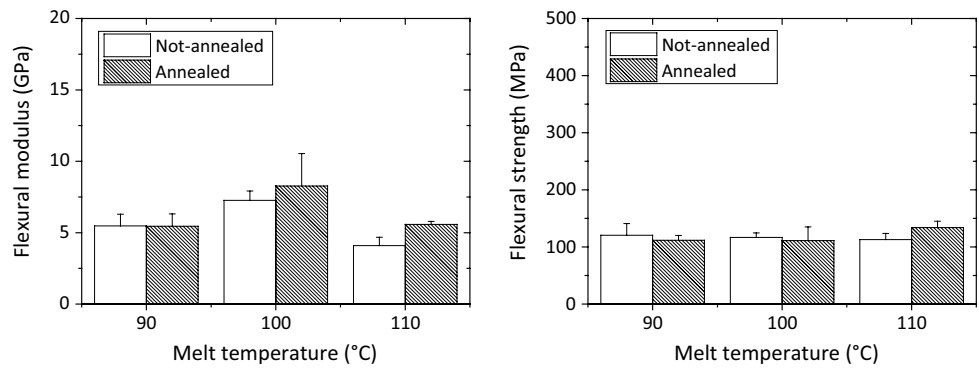
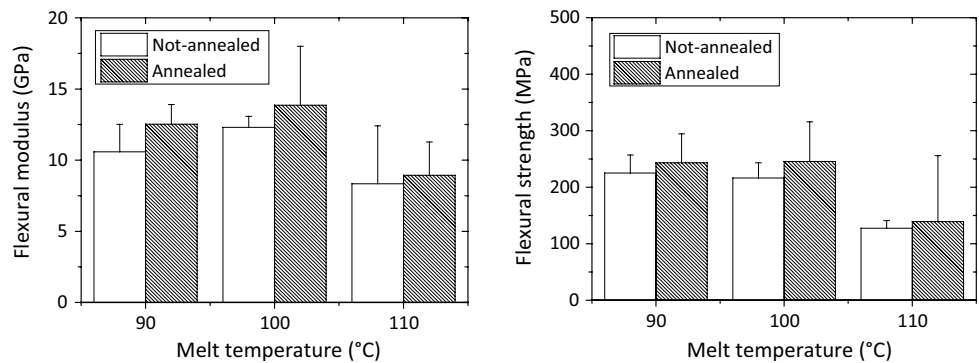


**Fig. 4** Effect of thermal annealing on the flexural modulus (left) and strength (right) of CF-PA6



### 3.2.3 CF-PA6

Table 2 presents the effect of thermal annealing on the fusion temperature and crystallinity of CF-PA6. Thermal annealing increased the fusion temperature by 4 °C at most. The crystallinity was close or less than that of the non-annealed CF-PA6 samples.

Figure 4 shows the flexural modulus and strength of CF-PA6. The flexural strength was improved by thermal annealing, while the crystallinity was not improved. The flexural modulus also increased by thermal annealing.

## 4 Discussion

Figure 5 plots the flexural modulus and strength of PA6, GF-PA6, and CF-PA6 against their crystallinity. Linear correlation lines were obtained. The flexural modulus and strength of PA6 correlated well with the crystallinity. This indicates that increasing the crystallinity improves the flexural modulus and strength. GF-PA6 showed less correlation between the flexural modulus and strength and the crystallinity. Meanwhile, the modulus and strength of CF-PA6 showed a negative correlation; they decreased as the crystallinity increased.

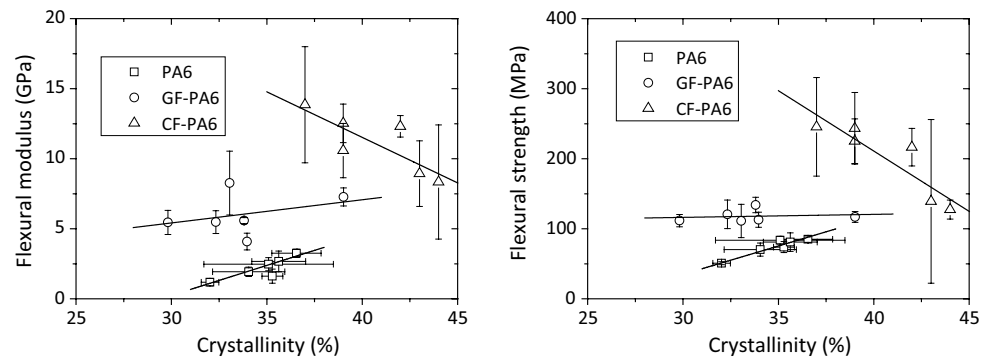
The flexural modulus and strength of PA6 showed a good correlation with the crystallinity. However, the

correlation became worse for both GF-PA6 and CF-PA6. This is not surprising if the moduli of GF and CF are considered. The typical flexural moduli of GF and CF are order of 10 and 100 GPa, respectively, which are 3 and 300 times higher than the flexural modulus of PA6 at 2.72 GPa (Brandrup et al. 2003). If the composite material consists of an amorphous phase, crystalline phase and reinforcing fibers, the volume percent of fiber has the greatest effect on the strength because it has the highest Young’s modulus among the three components. Therefore, increasing the crystallinity is less effective on the modulus and strength.

As noted previously, the crystallinity is an important property for a matrix polymer. However, its contribution to the mechanical properties of a composite is limited because the reinforcing materials (e.g., GF and CF) have a much higher Young’s modulus than the crystalline phase.

The Young’s modulus and strength of CF-PA6 showed a negative correlation against the crystallinity of PA6. This indicates that increasing the crystallinity decreases the flexural modulus. The crystallization of PA6 forms voids or residual stress on the CF surface. The formation of voids reduces the contact area of PA6 and CF. Eventually, they become stress concentration points for breaking. In situ polymerization of  $\epsilon$ -CL causes polymerization and crystallization to proceed simultaneously. Although controlling the crystallization independently is difficult, it is essential to lower the crystallinity for CF-PA6.

**Fig. 5** Relationship between the crystallinity of PA6, GF-PA6, and CF-PA6 and the flexural modulus (*left*) and strength (*right*)



## 5 Conclusion

The RTM process with in situ polymerization of  $\epsilon$ -CL was performed to prepare PA6, GF-PA6, and CF-PA6. The melt temperature for the RTM process increased the conversion and molecular weight. Thermal annealing increased the crystallinity of PA6 and the flexural modulus and strength. However, thermal annealing was less effective at improving the crystallinity, flexural modulus, and strength of GF-PA6 and CF-PA6. A negative correlation was observed between the crystallinity and flexural modulus and strength for CF-PA6.

## References

- Ben G, Hirabayashi A, Sakata K, Nakamura K, Hirayama N (2015) Evaluation of new GF RTP and CF RTP using epsilon caprolactam as matrix fabricated with VaRTM. *Sci Eng Compos Mater* 22:633–641
- Blaine RL (2002) thermal applications note polymer heats of fusion. TN048, TA Instruments
- Brandrup J, Immergut EH, Grulke EA (2003) *Polymer handbook*, 4th edn. Wiley, Amsterdam
- Castro JM, Macosko CW (1980) *SPE Technical Papers* 26:434
- Durin A, Boyard N, Bailleul JL, Billon N, Chenot JL, Haudin JM (2017) Semianalytical models to predict the crystallization kinetics of thermoplastic fibrous composites. *J Appl Polym Sci* 134:44508
- Haspel B, Hoffmann C, Elsner P, Weidenmann KA (2015) Characterization of the interfacial shear strength of glass-fiber reinforced polymers made from novel RTM processes. *Int J Plast Technol* 19:333–346
- Ito H, Tsutsumi Y, Minagawa K, Takimoto J, Koyama K (1995) Simulations of polymer crystallization under high pressure. *Colloid Polym Sci* 273:811–815
- Kamal MR, Ryan ME (1980) The behavior of thermosetting compounds in injection molding cavities. *Polym Eng Sci* 20:859–867
- Li H, Wang Y, Zhang C, Zhang B (2016) Effects of thermal histories on interfacial properties of carbon fiber/polyamide 6 composites: thickness, modulus, adhesion and shear strength. *Compos Part A Appl Sci Manuf* 85:31–39
- Pillay S, Vaidya UK, Janowski GM (2005) Liquid molding of carbon fabric-reinforced nylon matrix composite laminates. *J Thermoplast Compos Mater* 18:509–527
- Shojaei A, Ghaffarian SR, Karimian SMH (2003) Modeling and simulation approaches in the resin transfer molding process: a review. *Polym Compos* 24:525–544
- Taki K, Shoji N, Kobayashi M, Ito H (2016) A kinetic model of viscosity development for in situ ring-opening anionic polymerization of  $\epsilon$ -caprolactam. *Microsyst Technol* pp 1–9
- van Rijswijk K, Bersee HEN (2007) Reactive processing of textile fiber-reinforced thermoplastic composites: an overview. *Compos. Part A Appl Sci Manuf* 38:666–681
- Yan X, Imai Y, Shimamoto D, Hotta Y (2014) Relationship study between crystal structure and thermal/mechanical properties of polyamide 6 reinforced and unreinforced by carbon fiber from macro and local view. *Polymer* 55:6186–6194
- Zheng LY, Wang YL, Wan YZ, Zhou FG, Dong XH (2002) Preparation and properties of in situ polymerized fiber-reinforced nylon composites. *J Mater Sci Lett* 21:987–989